A ray theory approach to investigate the influence of flow velocity profiles on transit times in ultrasonic flow meters for gas and liquid

Kjell-Eivind Frøysa [a], Per Lunde [a] and Magne Vestrheim [b]

[a] Christian Michelsen Research AS, P.O. Box 6031 Postterminalen, N-5892 Bergen, Norway
[b] University of Bergen, Dept. of Physics, Allégaten 55, N-5007 Bergen, Norway

ABSTRACT

USM technology is today recognized as a competitive alternative for fiscal flow metering of gas, and is also considered for fiscal metering of oil and petroleum products. However, there are un-exploited potentials to reduce systematic errors, achieve higher accuracy, and to improve measurement traceability, giving perspectives for further development of the technology. The paper addresses the influences of flow velocity profile effects on transit times (sound refraction) and consequences for the measured flow velocity and sound velocity (VOS) in a USM. Systematic effects of axial and transversal flow velocity profiles at different Reynolds numbers and under various installation conditions are investigated using a ray propagation model with CFD calculated flow profiles as input. It has been found that for a wide range of axial and transversal profiles the measured flow velocity is not influenced significantly by sound refraction effects, except for relatively high flow velocities, assumed that compensation for uniform transversal flow is made (by configuration or software). Similarly, the measured VOS is not affected severely by sound refraction for a wide range of symmetrical and asymmetrical axial profiles, except for relatively high flow velocities. However, refraction effects due to transversal flow are significant also at more moderate velocities, and correction of current USM expressions may be needed for accurate VOS measurement.

1. INTRODUCTION

Multipath ultrasonic flow meters (USM) have demonstrated their capabilities to provide accurate and reliable fiscal metering of gas and liquid, within national regulations. For natural gas, better than ±0.7 % uncertainty (of measured value) is being reported [1-3], as required for custody transfer in large commercial pipelines [4,5]. For USM measurement of oil and petroleum products, ±(0.15-0.25) % uncertainty is claimed [6], based on *in-situ* flow calibration (prover).

Even within such high accuracy figures, demonstrated in flow testing, systematic errors may over time accumulate to significant economic values. Moreover, in service, conditions may be different from the test situation, and practical problems may occur so that occasionally it may be difficult to ensure that the above accuracy figures are actually reached. One challenge is now to be able to be confident of the in-service performance over a significant period of time and changing operational conditions [7]. USM technology is relatively young compared with more traditional flow metering technologies, and potentials and needs exist for further development, such as with respect to:

- Improved robustness, reliability and cost/benefit ratio,
- Improved understanding and exploitation the USM measurement principle (e.g. reduction of systematic effects, improved accuracy and traceability to international standards),
- Extended applications (density and calorific value measurement [8], wet gas metering [9], etc.).

Such developments require improved solutions within several technology areas related to the USM. Table 1 gives an overview of some effects which may influence on USM fiscal metering of gas,

assumed that the meter otherwise functions according to manufacturer recommendations. Flow calibration of the USM may eliminate or reduce a number of the systematic effects, but, as indicated in the table, several effects may still be influent, despite flow calibration [10,11].

Table 1. Uncertainty contributions to USM in field operation, with respect to volumetric flow rate measurement.

Uncertainty group	**Type of effect**	**Uncertainty contribution (examples)**	**Eliminated by flow calibration?** [a)]
Integration method (installation effects)	Systematic	• Pipe bend configurations upstream USM (possible difference re. flow calibr) • In-flow profile to upstream pipe bend (possible difference re. flow calibr.) • Meter orientation relative to pipe bends (possible difference re. flow calibr.) • Possible use of flow conditioners (difference re. flow calibration) • Possible wall corrosion, wear, pitting (influence on flow profiles) • Possible wall deposits, contamination (influence on flow profiles) • Initial wall roughness (influence on flow profiles)	Eliminated
Meter body	Systematic	• Measurement uncertainty of dimensional quantities (at "dry calibration") • Out-of-roundness • *P & T* effects on dimensional quantities (incl. possible *P & T co*rrections)	Eliminated Eliminated
Transit times	Systematic	• Cable/electronics/transducer/diffraction delay (*P*, *T* & flow effects, drift) • *Δt*-correction (*P* & *T* effects, drift) • Possible cavity delay correction • Possible deposits/liquid at transducer front • Sound refraction (flow profile effects on transit times) • Possible beam reflection at the pipe wall	Eliminated
	Random (repeata-bility)	• Turbulence (transit time fluctuations due to velocity & temperature fluct.) • Incoherent noise (due to RFI, pressure control valves, etc.) • Coherent noise (due to acoustic cross-talk, reverberation, etc.) • Finite clock resolution	

[a)] For flow calibrated USMs only uncertainties due to *changes of conditions from flow calibration to field operation* are in question.

For several of these effects, better control could be achieved if better understanding and a more solid theoretical basis for the USM methodology was available. The expressions forming the basis for present-day USMs are based on a number of assumptions which are not fulfilled in practice, such as uniform axial flow (i.e. infinite Reynolds number, *Re*), uniform or no transversal flow, interaction of infinitely thin acoustic beams (rays) with the flow, and simplified (if any) treatment of diffraction effects [10,12]. In reality, the axial flow profile will change both with *Re* and with the actual installation conditions (such as bend configurations, use of flow conditioner, wall corrosion, wear, pitting, deposits, etc.). Transversal flow is usually significant and non-uniform (swirl, cross-flow, etc.). Moreover, in reality the acoustic beam has a finite beam width, interacting with the flow over a finite volume, and with acoustic diffraction effects (due to finite transducer aperture). All of these factors influence on the USM integration method as well as the measured transit times. In order to further improve the USM theoretical basis, there is a need to investigate the significance of such factors on the USM performance, and - for the significant effects - to find methods to reduce or correct for such effects.

In particular, in today's USM transit time expressions, a simplified model is used to account for the flow profiles of Reynolds numbers to be met in practice, and the influence of asymmetrical axial and non-uniform transversal flow profiles found in typical metering stations. Systematic transit time effects due to refraction of sound propagating through the non-uniform fluid flow will influence both on the measured flow velocity and the sound velocity (VOS). Traditionally, the VOS measured by the USM has been used for self-check of the USM, and as possible input to the VOS correction of vibrating-element gas densitometers used in mass flow measurement. In addition, recent developments have shown that it can be used as a basis for calculation of density and calorific value of natural gas [8]. Through the VOS, therefore, a USM supplied with such (meter independent) software can be used (with more limited accuracy) as a mass flow meter and an energy flow meter,

in addition to its traditional use as a volumetric fiscal flow meter. In such new applications, a VOS measurement uncertainty of about ±0.25 m/s (±0.06 %) or better would be needed (among others) for sales metering of density or calorific value [13]. In less critical applications such as allocation and check metering, a less accurate VOS measurement is acceptable. This means that control with the accuracy of the VOS measurement made in the USM is now of even higher importance than a few years ago.

As one step towards better understanding, control and an improved USM methodology, the present paper addresses the inaccuracies made when using the traditional USM transit time expressions in the range of flow profiles for Reynolds numbers relevant for liquid and gas flow, and under conditions of disturbed flow profiles (different pipe bend configurations). The accuracy of the traditional expressions used for measurement of flow velocity and VOS is investigated by use of acoustic ray theory, with respect to flow profile effects on transit times (sound refraction). Axial and transversal flow profiles calculated using computational fluid dynamics (CFD) modelling of pipe flow are used as input to the ray propagation model. The ray theory simulations are compared with the traditional transit-time expressions used in today's USMs, derived for the simplified case of uniform axial and uniform or no transversal flow. The resulting deviations in flow velocity and VOS for the traditional USM functional relationships due to sound refraction, are evaluated and discussed. Limitations of the approach used here are addressed in Section 6.

2. CURRENT USM METHODOLOGY - THEORETICAL BASIS

The present section summarizes the basic and well-known expressions used in current USMs, as a basis for the improved USM ray theory that is described and compared to in Sections 3-5. The description covers USMs with non-reflecting (cf. Fig. 1) [1,2,6] as well as reflecting path [3] configurations, in the same formalism.

A USM measures the axial (x) component of the volumetric flow rate at line conditions (with respect to pressure, temperature and fluid quality), q_v, defined as (for fixed time, $t = t_0$) [12]

$$q_v = \iint_A v_x(x_0, y, z, t_0)\, dy\, dz \quad , \tag{1}$$

where A is the cross sectional area of the pipe (in the y, z - plane, at $x = x_0$ = constant), and v_x is the axial (x) component of the flow velocity. For circular cross-section, the double integral in Eq. (1) can be written as a single integral, e. g. [12,14],

$$q_v = \int_{-R}^{R} \int_{-\sqrt{R^2-y^2}}^{\sqrt{R^2-y^2}} v_x(x_0, y, z, t_0)\, dz\, dy = 2 \int_{-R}^{R} \sqrt{R^2 - y^2}\, \bar{v}_x(y)\, dy \,, \tag{2}$$

where $R = D/2$ is the inner radius of the pipe and

$$\bar{v}_x(y) = \frac{1}{2\sqrt{R^2 - y^2}} \int_{-\sqrt{R^2-y^2}}^{\sqrt{R^2-y^2}} v_x(x_0, y, z, t_0)\, dz \tag{3}$$

is the average axial flow velocity (the line integral) over the chord with lateral position y. For calculation of q_v by numerical integration, Eq. (2) is approximated by

$$q_v \approx \pi R^2 \sum_{j=1}^{N_C} w_j^c \overline{v}_{j,x}^c \ , \tag{4}$$

where N_c is the number of chords (e.g. 4-5 and 9 for non-reflecting [1,2,6] and reflecting path USMs [3], respectively). w_j^c is the integration weight factor of chord no. j, and $\overline{v}_{j,x}^c = \overline{v}_x(y_j)$ is the average axial flow velocity over chord no. j, which is located at $y = y_j$, $j = 1,\ldots, N_c$.

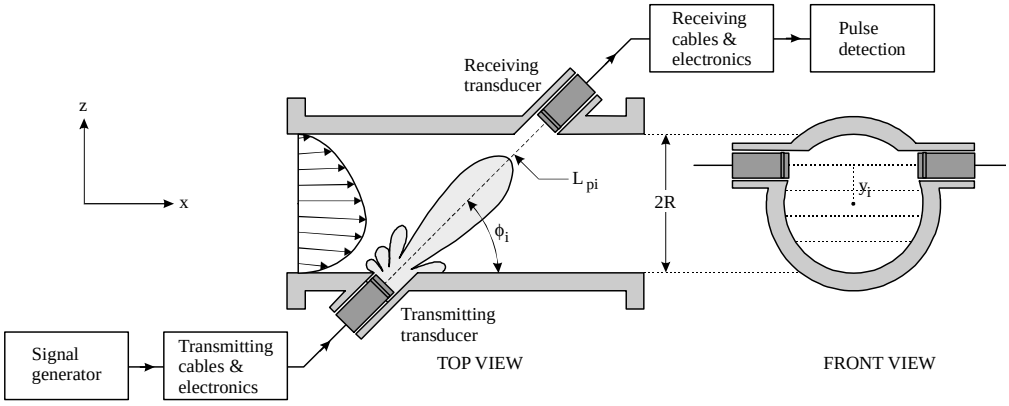

Fig. 1. Schematic illustration of a single path (no. i) in a USM with non-reflecting paths (parallel chords) (for downstream sound propagation). (Left: centre path example ($y_i = 0$); Right: path at lateral chord position y_i.).

In USMs for fiscal metering, non-reflecting as well as reflecting-path configurations are in use [1-3,6]. The flow velocity is measured over N acoustic paths (typically 4-6), having inclination angles ϕ_i to the axial flow direction of typically 40° to 60°, cf. Fig. 1 [12,14]. Note that the number of chords is not necessarily the same as the number of acoustic paths, since two paths can have the same projection into the pipe cross section, and also since a reflecting path can correspond to more than one chord. For each path, transit times are measured electronically for high-frequency ultrasonic pulses propagating across the pipe, at an angle, ϕ_i, with respect to the pipe axis, downstream with the flow, and upstream against the flow. Ultrasonic transducers are used to transmit and receive the signals. For each acoustic path, the difference between the upstream and the downstream propagating transit times is proportional to the average flow velocity along the acoustic path. Multiple acoustic paths are used to sample the flow velocity profile in the pipe at a set of discrete chords, to improve the metering accuracy.

The measured upstream and downstream transit times of path no. i, $t_{1i}^{measured}$ and $t_{2i}^{measured}$, contain possible time delays due to signal propagation in the transmit and receive cables, electronics, transducers, diffraction effects, and possible cavities in front of the transducers, cf. Fig. 1. For acoustic path no. i, the measured transit times may be written as [12]

$$t_{1i}^{measured} = t_{1i} + t_{1i,0}^{eltr} + t_i^{cavity} \ , \tag{5a}$$

$$t_{2i}^{measured} = t_{2i} + t_{2i,0}^{eltr} + t_i^{cavity} = t_{2i} + t_{1i,0}^{eltr} - \Delta t_{i,0}^{corr} + t_i^{cavity} \quad , \qquad i = 1, \ldots, N \tag{5b}$$

where t_{1i} and t_{2i} are the upstream and downstream transit times along the interrogation length (cf. Fig. 2), $t_{1i,0}^{eltr}$ and $t_{2i,0}^{eltr}$ are the cable/electronics/transducer/diffraction time delay for upstream and downstream propagation, respectively, and $\Delta t_{i,0}^{corr} = t_{1i,0}^{eltr} - t_{2i,0}^{eltr}$ is the Δt-correction. t_i^{cavity} is the cavity delay of path no. i (if used), at line conditions. For transducers with the front centre point flush with the pipe wall, t_i^{cavity} is normally not used, i.e. $t_i^{cavity} = 0$ is assumed.

2.1 "Traditional approach"; uniform axial flow and no transversal flow

For the simplified case where the flow velocity profile is assumed to be uniform and purely axial (i.e. no transversal flow), the two transit times of path no. i for propagation over the interrogation length can be found by a simple geometrical approach as (see Fig. 2)

$$t_{1i} = \frac{(N_{refl,i}+1)L_i}{c_i - \bar{v}_{i,x}\cos\phi_i}, \qquad t_{2i} = \frac{(N_{refl,i}+1)L_i}{c_i + \bar{v}_{i,x}\cos\phi_i}, \tag{6}$$

where ϕ_i is the inclination angle of acoustic path no. i, $\bar{v}_{i,x}$ is the average axial flow velocity over the length L_i of the path, and c_i is the average sound velocity (VOS) over the length L_i. $N_{refl,i}$ is the number of reflections in path no. i. For USMs with non-reflecting paths ($N_{refl,i} = 0$), L_i is the interrogation length of path no. i (cf. Fig. 2a). For USM with reflecting paths ($N_{refl,i} > 0$), L_i is the portion of the distance from the transmitting transducer front to the first reflection point which is lying inside a cylinder formed by the meter body's inner diameter, cf. Fig. 2b. (This length is $1/(N_{refl,i}+1)$ of the the interrogation length of path no. i.)

From Eqs. (6), c_i can be eliminated, giving

$$\bar{v}_{i,x} = \frac{(N_{refl,i}+1)L_i(t_{1i} - t_{2i})}{2t_{1i}t_{2i}\cos\phi_i}. \tag{7}$$

Alternatively, a more sophisticated and accurate ray tracing approach can be taken, as reported by McCartney *et al*. [15], leading to (when including the factor $(N_{refl,i}+1)$ for reflecting-path USMs)

$$t_{1i} = \frac{(N_{refl,i}+1)L_i}{\sqrt{c_i^2 - \bar{v}_{i,x}^2 \sin^2\phi_i} - \bar{v}_{i,x}\cos\phi_i}, \qquad t_{2i} = \frac{(N_{refl,i}+1)L_i}{\sqrt{c_i^2 - \bar{v}_{i,x}^2 \sin^2\phi_i} + \bar{v}_{i,x}\cos\phi_i}, \tag{8}$$

as an extension to Eq. (6). Eqs. (8) are claimed by McCartney *et al*. to be valid also for non-uniform axial flow velocity profiles. However, an underlying assumption in their analysis is that the rays are straight lines. This is possible for the uniform axial flow profile only, and Eqs. (8) are therefore derived only for uniform axial and no transversal flow [14,12].

It is interesting to note that Eqs. (8) lead to exactly the same expression, given by Eq. (7), for the average flow velocity over the acoustic path, $\bar{v}_{i,x}$, as the simplified geometrical approach described above (Eq. (6)) and illustrated in Fig. 2.

Eqs. (8) also lead to the well-known expression for the sound velocity, e.g. [12,14],

$$c_i = \frac{(N_{refl,i}+1)L_i\sqrt{(t_{1i}+t_{2i})^2\cos^2\phi_i + (t_{1i}-t_{2i})^2\sin^2\phi_i}}{2t_{1i}t_{2i}\cos\phi_i}, \tag{9}$$

which is "exact" (within the ray approximation) for uniform axial flow and no transversal flow. For transversal flow as well as for other axial profiles it represents an approximation (cf. Section 6).

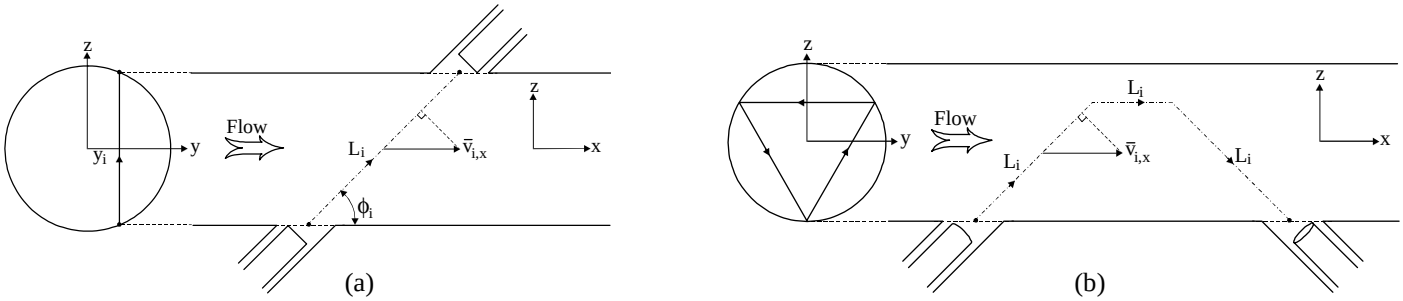

Fig. 2. Schematic illustration of the "traditional approach" for path no. *i* in the USM, accounting for *uniform axial flow and no transversal flow*. (a) Non-reflecting path ($N_{refl,i}$ = 0); (b) Reflecting path (example with $N_{refl,i}$ = 2).

2.2 "Extended traditional approach", accounting for uniform transversal flow

By a simple analysis, it is possible to extend the above analysis one step towards more realistic conditions, by including effects of uniform transversal flow.

In a real flow metering situation, there will be transversal flow velocity components in addition to the axial flow velocity component. Such transversal flow velocity components influence on the transit times, and on the measured axial flow and VOS. In the simplest approximation, the axial and transversal flow profiles are both considered to be uniform. A simple, geometrical approach can again be taken, giving the following upstream and downstream transit times (see Fig. 3) [8]:

$$t_{1i} = \frac{(N_{refl,i}+1)L_i}{c_i - \bar{v}_{i,x}\cos\phi_i - \bar{v}_{i,T}\sin\phi_i}; \qquad t_{2i} = \frac{(N_{refl,i}+1)L_i}{c_i + \bar{v}_{i,x}\cos\phi_i + \bar{v}_{i,T}\sin\phi_i}, \tag{10}$$

where $\bar{v}_{i,T}$ is the average transversal flow velocity component along the chord in question, i.e. in the plane spanned by the path direction and the *x*-axis. For non-reflecting path USMs with parallel chords, this is the *x*-*z* plane, so that $\bar{v}_{i,T} = \bar{v}_{i,z}$, cf. Fig. 3a. For USMs with reflecting paths, this plane changes along the path, cf. Fig. 3b. In both cases Eqs. (10) represent an extension to Eqs. (6) by accounting for uniform transversal flow through the term $\bar{v}_{i,T}\sin\phi_i$. Note that in this traditional USM theory, the small transversal-flow normal component to $\bar{v}_{i,T}$ is neglected (i.e. $\bar{v}_{i,y}$ for non-reflecting path USMs).

From Eqs. (10), c_i can be eliminated, giving [8]

$$\bar{v}_{i,x} + tan\phi_i \bar{v}_{i,T} = \frac{(N_{refl,i}+1)L_i(t_{1i}-t_{2i})}{2t_{1i}t_{2i}\cos\phi_i}, \tag{11}$$

as an extension and improvement relative to Eq. (7). In current fiscal flow meters, Eqs. (7) or (11) (for flow velocity) and Eq. (9) (for sound velocity) are expressions in use to obtain the average axial flow velocity and VOS at acoustic path no. *i*.

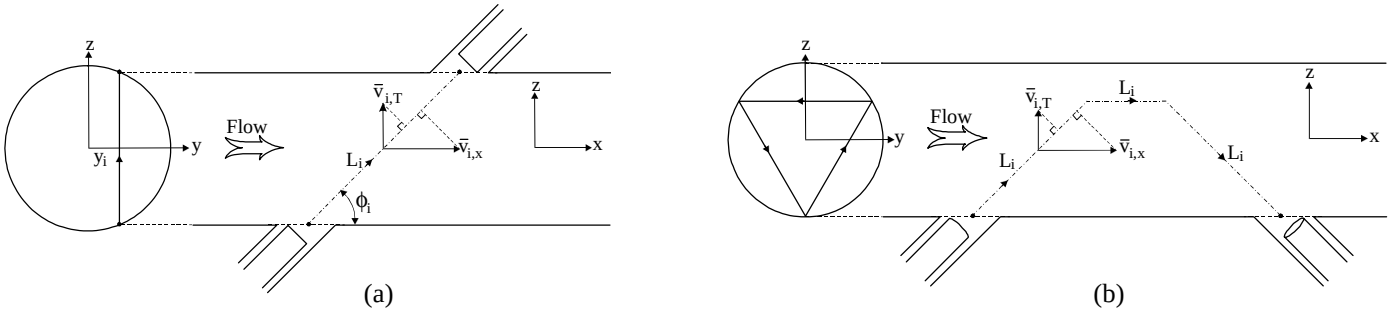

Fig. 3. Illustration of the "extended traditional approach" for path no. *i* in the USM, accounting for *uniform axial and uniform transversal flow*. (a) Non-reflecting path ($N_{refl,i} = 0$); (b) Reflecting path (example with $N_{refl,i} = 2$).

2.3 Associating paths with chords, and path configuration

In Eq. (4), the average axial flow velocity over chord no. *j*, $\bar{v}^c_{j,x}$, is needed, whereas in Eqs. (7) and (11) the average axial flow velocity over the length L_i of the inclined path no. *i*, $\bar{v}_{i,x}$, is involved. It is usual to assume that these two quantities are approximately equal,

$$\bar{v}^c_{j,x} \approx \bar{v}_{i,x}, \tag{12}$$

for corresponding chords and acoustic paths. Hence, in this approximation it is assumed that the axial flow velocity profile is constant over the length of the USM. It is also usual to write Eq. (4) as

$$q_v \approx \pi R^2 \sum_{j=1}^{N_C} w^c_j \bar{v}^c_{j,x} \approx \pi R^2 \sum_{i=1}^{N} w_i \bar{v}_i \ , \tag{13}$$

where

$$\bar{v}_i = \frac{(N_{refl,i}+1)L_i(t_{1i}-t_{2i})}{2t_{1i}t_{2i}\cos\phi_i} \tag{14}$$

is the average axial flow velocity which is measured by the USM at path no. *i*, and w_i is the integration weight of the path. However, from Eq. (11) it appears that Eq. (14) does not in general yield the measurand $\bar{v}_{i,x}$. Two approaches are in use today to compensate for the error in $\bar{v}_i$ which is caused by e.g. transversal flow:

(a) The geometrical path configuration (including ϕ_i, w_i and $N_{refl,i}$, $i = 1, \ldots, N$) is chosen to reduce the influence of the types of transversal flow of main interest in ultrasonic flow metering, on the integration method of the USM.

(b) Approach (a), in combination with active use of Eq. (11) and an estimate of the average transversal flow at path no. $i, \bar{v}_{i,T}$, for paths without transversal flow cancellation by configuration.

In the case where there is one acoustic path per chord, so that $N = N_c$, the path weights w_i are equal to the chord weights w_j^c. In the case where there are 2 acoustic paths per chord (for all or some of the chords), the relation between the weights w_i, $i = 1, ..., N$ and w_j^c, $j = 1, ..., N_c$ will be more complex. It should also be noted that for non-reflecting paths, it is only when there are 2 acoustic paths per chord for every chord, i.e. $N = 2N_c$, that the transversal flow velocity component $\bar{v}_{i,T}$ in Eq. (11) will be cancelled for any transversal flow profile. For a smaller number of acoustic paths, only certain transversal flow velocity profiles will in general be cancelled.

3. RAY THEORY MODEL FOR SOUND PROPAGATION IN NON-UNIFORM PIPE FLOW

The traditional expressions on which today's USMs are based, given by Eqs. (7) or (11) (for flow velocity) and Eq. (9) (for VOS), are based on assumptions of uniform axial and uniform (or no) transversal flow velocity profiles, as explained above. In real flow, neither the axial nor the transversal flow profiles are uniform, and the traditional expressions represent approximations. To account for sound refraction caused by the non-uniform profiles at finite *Re* numbers and disturbed flow conditions, an improved ray theory model relative to McCartney *et al.*'s approach has been developed. In this theory, the influence of non-uniform as well as asymmetrical axial and transversal flow on the transit times can be investigated. The model is a further development of earlier work by the authors, cf. [14,16].

The model used here is based on the ray-tracing equations for a moving medium as formulated by Pierce [17] (which are equivalent to those given by Lighthill [18]):

$$\frac{d\underline{s}}{dt} = -\underline{s}\cdot\nabla\underline{v} - \underline{s}\times\nabla\times\underline{v} - \frac{1-\underline{v}\cdot\underline{s}}{c}\nabla c\,, \qquad \frac{d\underline{x}}{dt} = \underline{v} + \frac{c^2\,\underline{s}}{1-\underline{v}\cdot\underline{s}}\,, \tag{15}$$

where $\underline{s}$ is the wave slowness vector, t is the time, $\underline{x}(t)$ describes the ray trajectory, and $\underline{v}(\underline{x}) = (v_X(x,y,z), v_Y(x,y,z), v_Z(x,y,z))$ is the flow velocity vector. For simplicity in notation, the subscript "i" for path no. i is omitted here. In addition to the ray approximation, which in the present work is basically a high-frequency approximation where the beam is described as an infinitely thin ray, and diffraction effects are neglected (cf. Fig. 4), the following assumptions are made: (a) Constant velocity of sound, c, (b) 2-dimensional flow: $v_Y = 0$, and (c) v_X and v_Z are independent of x and y: $v_X = v_X(z)$, $v_Z = v_Z(z)$.

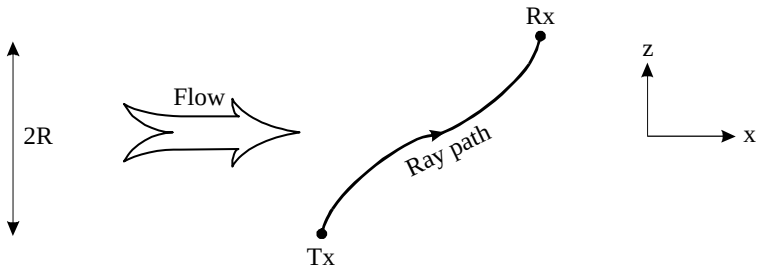

Fig. 4. Principle sketch of the ray path from the transmitting transducer (Tx) to the receiving transducer (Rx), for downstream propagation in acoustic path no. *i*.

None of these three assumptions represent severe limitations, cf. Section 6. Assumption (c) means that the flow profile is taken to be constant over the length of the USM.

Under these assumptions, Eqs. (15) reduce to the set of four coupled differential equations

$$\frac{ds_x}{dt} = 0\,, \qquad \frac{ds_z}{dt} = -s_x \frac{\partial v_x}{\partial z} - s_z \frac{\partial v_z}{\partial z}\,, \tag{16a}$$

$$\frac{dx}{dt} = v_x(z) + \frac{c^2 s_x}{1 - v_x(z)s_x - v_z(z)s_z}\,, \qquad \frac{dz}{dt} = v_z(z) + \frac{c^2 s_z}{1 - v_x(z)s_x - v_z(z)s_z}\,. \tag{16b}$$

In order to integrate Eqs. (16), initial conditions are specified at $t = 0$. For downstream propagation, these initial conditions are, for $x = 0$ and $z = -R$,

$$s_x = \frac{\cos\varphi}{c + v_x(-R)\cos\varphi + v_z(-R)\sin\varphi}\,, \qquad s_z = \frac{\sin\varphi}{c + v_x(-R)\cos\varphi + v_z(-R)\sin\varphi}\,. \tag{17}$$

For upstream sound propagation, modified but similar initial conditions are used (expressions not given here). From the set of differential equations given by Eqs. (16), with initial conditions given by Eqs. (17), the ray paths and transit times have been calculated numerically using a fourth order Runge-Kutta method. 3-dimensional numerical CFD calculations of v_x, v_y and v_z (axial and transversal flow profiles, respectively) have been used as input to Eqs. (16), in combination with cubic spline interpolation between the CFD mesh points, cf. Section 4. An iteration procedure to determine the initial ray angle φ based on Newton's method has been used to ensure that the ray ends at the specified receiver point. A non-uniform time step along the path is used, with 3 regions, and a total of typically 30000 time steps per path. The time steps are typically 10^{-9} s close to the wall, and increase into the pipe. Note that the present approach gives the ray paths and transit times, t_{1i} and t_{2i}, but not ray amplitudes.

4. CFD FLOW PROFILE CALCULATIONS

3-dimensional flow velocity profiles have been calculated using the CFD-code *MUSIC* [19], for various USM installation conditions (pipe bends). The profiles are used in Section 5 as input to the numerical ray model described in Section 3. The following installation conditions have been used here:

- USM installed in long straight pipe, for various Reynolds numbers, see Fig. 5,
- USM installed 10D downstream a single 90° bend, see Fig. 6a,
- USM installed 10D downstream a double 90° bend out of plane, see Fig. 6b.

4.1 Straight pipe, Reynolds number variation

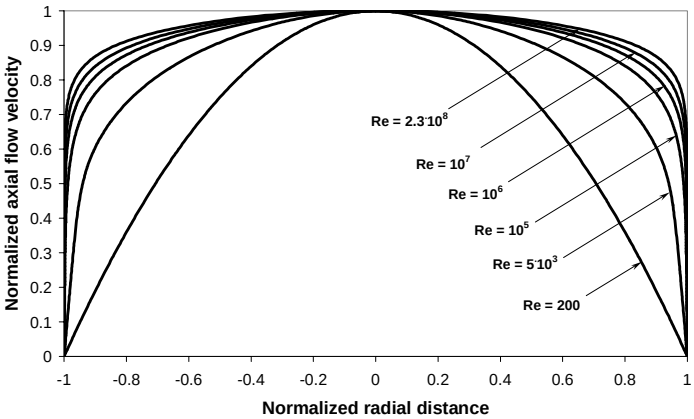

Fig. 5. Axial flow velocity profiles for a straight pipe, calculated for different Reynolds numbers using CFD.

Fig. 5 shows 3-dimensional (symmetrical) axial flow profiles for a straight pipe with smooth wall, calculated for a series of Reynolds numbers in the range Re = 200-$2.3\cdot10^8$ using the CFD model. For oil and gas, the relevant Reynolds number ranges are about Re = 10^2-10^6 and $5\cdot10^5$-10^8, respectively. In ideal straight pipe flow, the transversal flow vanishes, and the axial flow velocity profile is symmetrical. The well-known dependency of the profile flatness on the Reynolds number, which is demonstrated in the figure, means that

a variety of different flow profiles have to be taken into account in the discussion of sound refraction effects on transit times, flow velocity and VOS, even for the "simple" case of a straight pipe. The CFD calculations of axial profiles have been compared with experimental profiles for fully developed flow, including (for the range $Re = 7 \cdot 10^3$-10^7) published results from Princeton (Superpipe), Erlangen, Melbourne, Delft facilities and others, with reasonable agreement [19], similar to such comparisons published elsewhere.

4.2 Pipe with bends (installation effects)

Fig. 6 shows 3-dimensional axial and transversal flow velocity profiles 10D downstream a single 90° bend and a double 90° bend out of plane, calculated using the CFD model.

In these calculations the bend inlet-flow conditions were taken to be a power law axial profile with $Re = 10^5$ and no transversal flow. The axial profiles are typically asymmetrical downstream such bend configurations. The transversal profiles are typically of cross flow and swirl type for the single and double bend configurations, respectively. The CFD calculations of axial and transversal profiles have been compared with published experimental and CFD calculated profiles [19]. The largest transversal flow components are more than 10 % of the axial component (both averaged over the path).

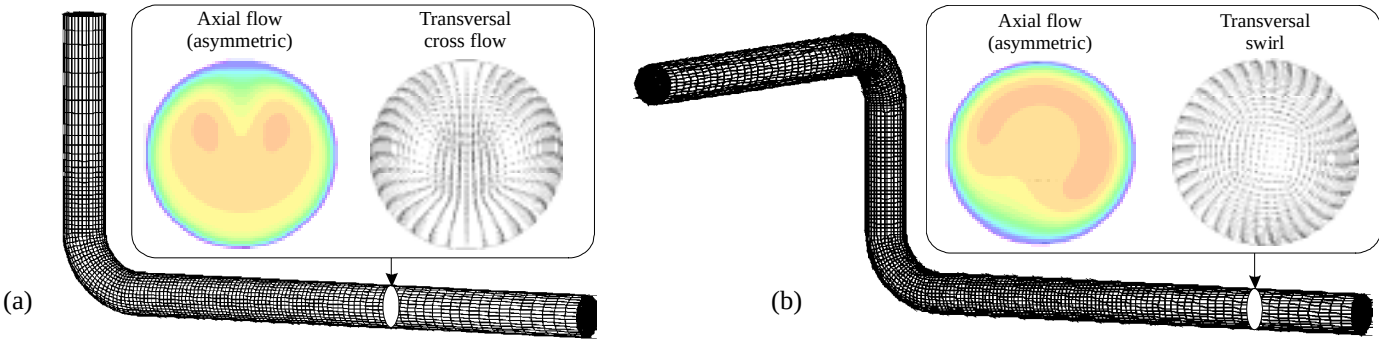

Fig. 6. 3-dimensional flow velocity profiles (axial and transversal) calculated 10D downstream a bend using CFD. (a) Single 90° bend, (b) Double 90° bend out-of-plane.

5. RAY THEORY RESULTS IN NON-UNIFORM AND DISTURBED FLOW

In the following, the traditional USM expressions, Eqs. (9) and (11), are tested for transit times calculated by ray theory, for more realistic axial and transversal flow than the uniform profiles for which they are derived. Using the CFD-calculated axial and transversal flow profiles for straight pipes (Fig. 5) and pipes with bends (Fig. 6) as input, numerical simulations of transit times have been made using the ray theory model for sound propagation described in Section 3. The following parameters have been used in the simulations: D = 0.3 m (≈ 12"), c_i = 400 m/s and ϕ_i = 45°.

The procedure used is as follows: Firstly, the reference values of $\bar{v}_{i,x}$ and $\bar{v}_{i,T}$ over path no. i are calculated by numerical integration of the CFD calculated profiles. Path transit times t_{1i} and t_{2i} are then calculated using the ray propagation model of Section 3. These transit times are inserted into Eq. (7) to obtain an estimate of $\bar{v}_{i,x}$, denoted $\bar{v}_{i,x}^{ray}$. With respect to the average axial flow velocity at the path, two deviations are then calculated and plotted: between $\bar{v}_{i,x}^{ray}$ and $\bar{v}_{i,x}$ (cf. Eq. (7)), and

between $(\bar{v}_{i,x}^{ray} - tan\phi_i \bar{v}_{i,T})$ and $\bar{v}_{i,x}$ (cf. Eq. (11)). With respect to VOS, t_{1i} and t_{2i} are inserted into Eq. (9) to obtain an estimate of c_i, denoted c_i^{ray}. The deviation between c_i^{ray} and c_i is then calculated and plotted.

5.1 Straight pipe: Symmetrical axial flow, effects of Reynolds number variation

In the case of a uniform axial flow profile, and no transversal flow (as is an underlying assumption behind Eqs. (7) and (9)), the ray path between the transmitter and the receiver will be the straight line. Non-uniformity in the axial flow profile will cause the ray path to deviate from this straight line.

In Fig. 7, the ray paths are shown for a flow velocity of 50 m/s, for a laminar (parabolic) axial flow profile (*Re* = 200, (a)) and a turbulent flow profile (*Re* = 5000, (b)). The two profiles are shown in Fig. 5. In the case of the laminar flow profile, the deviation of the ray path from the straight line is larger than for the turbulent flow profile. This is because the turbulent flow profile is closer to a uniform flow profile (which gives a straight line) than the laminar profile.

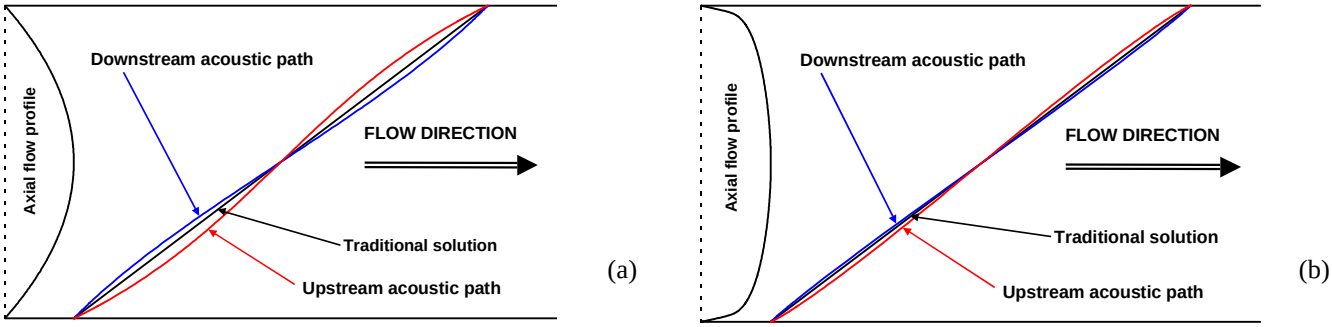

Fig. 7. Calculated acoustic ray paths for upstream and downstream propagation, for two types of axial flow profiles in an ideal straight pipe (no transversal flow), calculated using CFD. Here, ϕ = 45°, c = 400 m/s, D = 30 cm, and v_x = 50 m/s. (a) Laminar (parabolic) axial flow profile (*Re* = 200), (b) Turbulent axial flow profile (*Re* = 5000).

The deviation of the ray path from a straight line (caused by sound refraction) will also influence on the upstream and downstream transit times of the path. This will again affect the flow velocity and VOS measured over the acoustic path, as shown in Fig. 8. The figure shows the deviation using Eq. (7) (or equivalently, Eq. (11)) (left part) and Eq. (9) (right part), for a centre path in a USM, when the transit times are calculated by ray theory using the non-uniform axial flow velocity profiles as input. The deviations are shown for the six Reynolds numbers in the range 200-2.3·10^8 given in Fig. 5 as well as 8.8·10^3, and flow velocities up to 50 m/s. However, it should be noted that not all combinations of Reynolds numbers and flow velocity shown in Fig. 8 are possible to obtain in practice in ultrasonic flow metering, but shown here for completeness. Today, multipath USMs for gas typically operate up to velocities in the range 30-40 m/s. This upper limit is continuously being pushed upwards, driven by market needs. Ultrasonic flare gas meters may operate at velocities approaching 150 m/s, tentatively.

For the refraction effect on the measured axial flow velocity, Fig. 8 shows that the *turbulent flow velocity profiles* studied here give a systematic deviation which is significant only for the (relatively rare) combination of high flow velocities and low Reynolds numbers. For example, 0.1 % deviation is found for $\bar{v}_{i,x}$ = 40 m/s and *Re* = 5000. The *parabolic profile* corresponding to laminar flow gives significantly larger deviation to the uniform flow profile solution. However, the parabolic flow velocity profile is of most relevance for liquid flow metering of very low Reynolds numbers (less

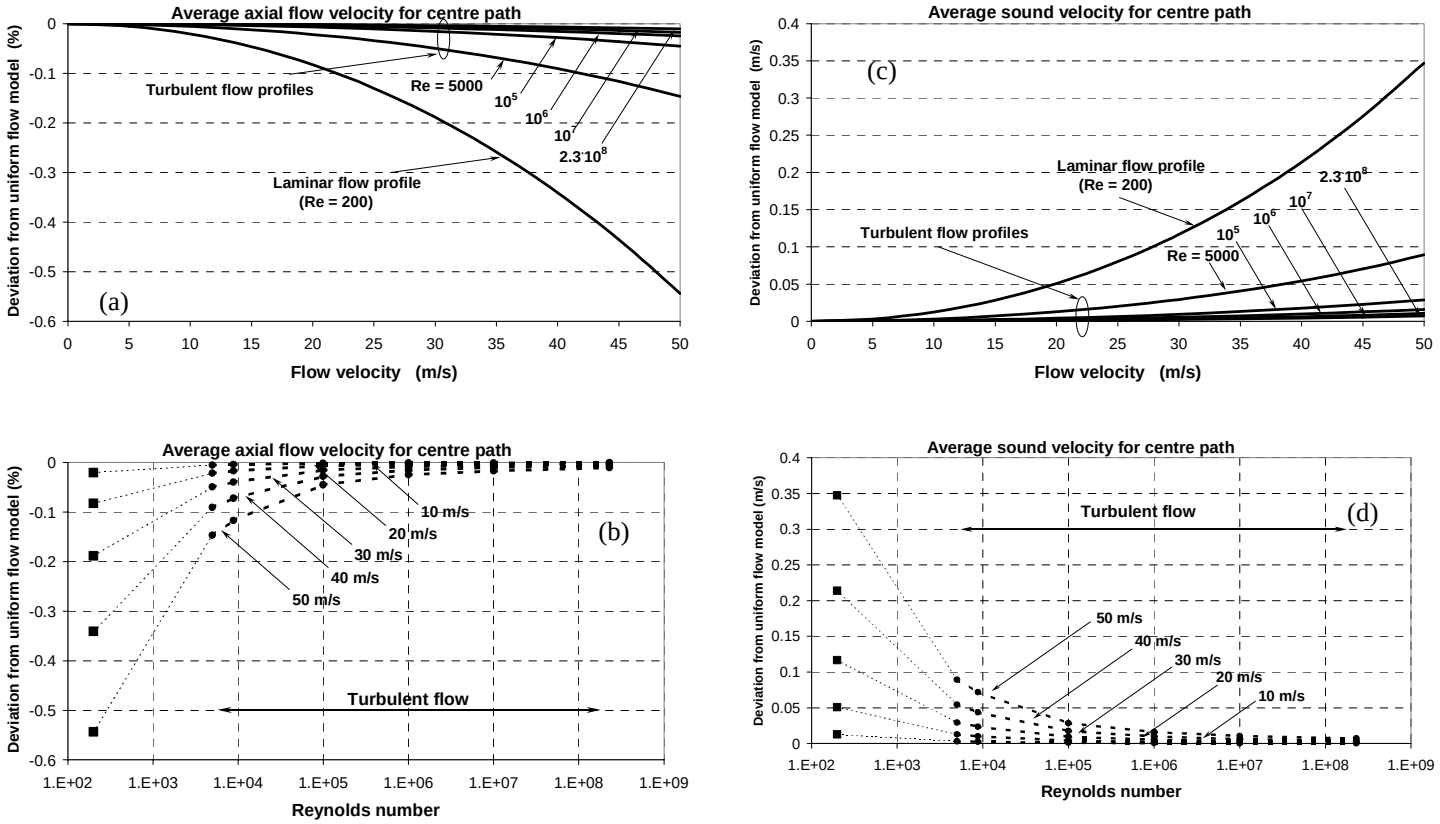

Fig. 8. The effect of non-uniform axial flow on the estimate of (left): the average axial flow velocity (deviation using Eq. (7) (or Eq. (11)), and (right): VOS (deviation using Eq. (9)), for a centre path, and for no transversal flow (ideal straight pipe flow). The upper and lower figures give the deviations plotted versus the average axial flow velocity and the Reynolds number, respectively.

than 10^3), for which high velocities are not so relevant unless for very high fluid viscosity and small pipe diameters.

For the refraction effect on the estimated VOS, Fig. 8 shows that the *turbulent flow velocity profiles* studied here give a systematic VOS deviation which is significant only for the (relatively rare) combination of very high flow velocities and low Reynolds numbers. For example, 0.05 m/s deviation is found for $\bar{v}_{i,x}$ = 40 m/s and *Re* = 5000. The *parabolic profile* gives significantly larger deviation to the uniform flow profile solution. However, as discussed above, high flow velocities may not be so relevant for the low Reynolds numbers in question for laminar flow.

From these straight pipe results, two parameters have been identified which, - for turbulent profiles, may be used as a quick and approximate evaluation of the importance of sound refraction due to symmetrical axial profiles on the measured flow velocity and VOS in a path, respectively:

$$P_v \equiv 30\frac{M_i}{\sqrt{ln\left(\frac{Re}{2000}\right)}}, \qquad P_c \equiv 90\frac{M_i}{ln\left(\frac{Re}{100}\right)}, \tag{18}$$

where $M_i = \bar{v}_{i,x}/c_i$ is the Mach number at path no. *i*. P_v and P_c can only be applied for *Re* > 5000 (turbulent flow). The deviation in flow velocity ($\bar{v}_{i,x}$) from Eq. (7) (or Eq. (11)) is less than 0.01 %

when $P_v < 1$. Similarly, the deviation in VOS (c_i) from Eq. (9) is found to be less than 0.0025 % when $P_c < 1$.

5.2 Single 90^o bend - Effects of asymmetrical axial and transversal flow

Fig. 9 shows the deviation from the reference values ($\overline{v}_{i,z}$ and c_i) by using Eqs. (7) and (11) (for flow velocity) and Eq. (9) (for VOS), for various lateral chord positions (y/R) and two meter orientations, when the transit times are calculated by ray theory using the CFD calculated profiles shown in Fig. 6a as input to the ray model. 0^o orientation is here taken to be normal to the inlet pipe of the last bend.

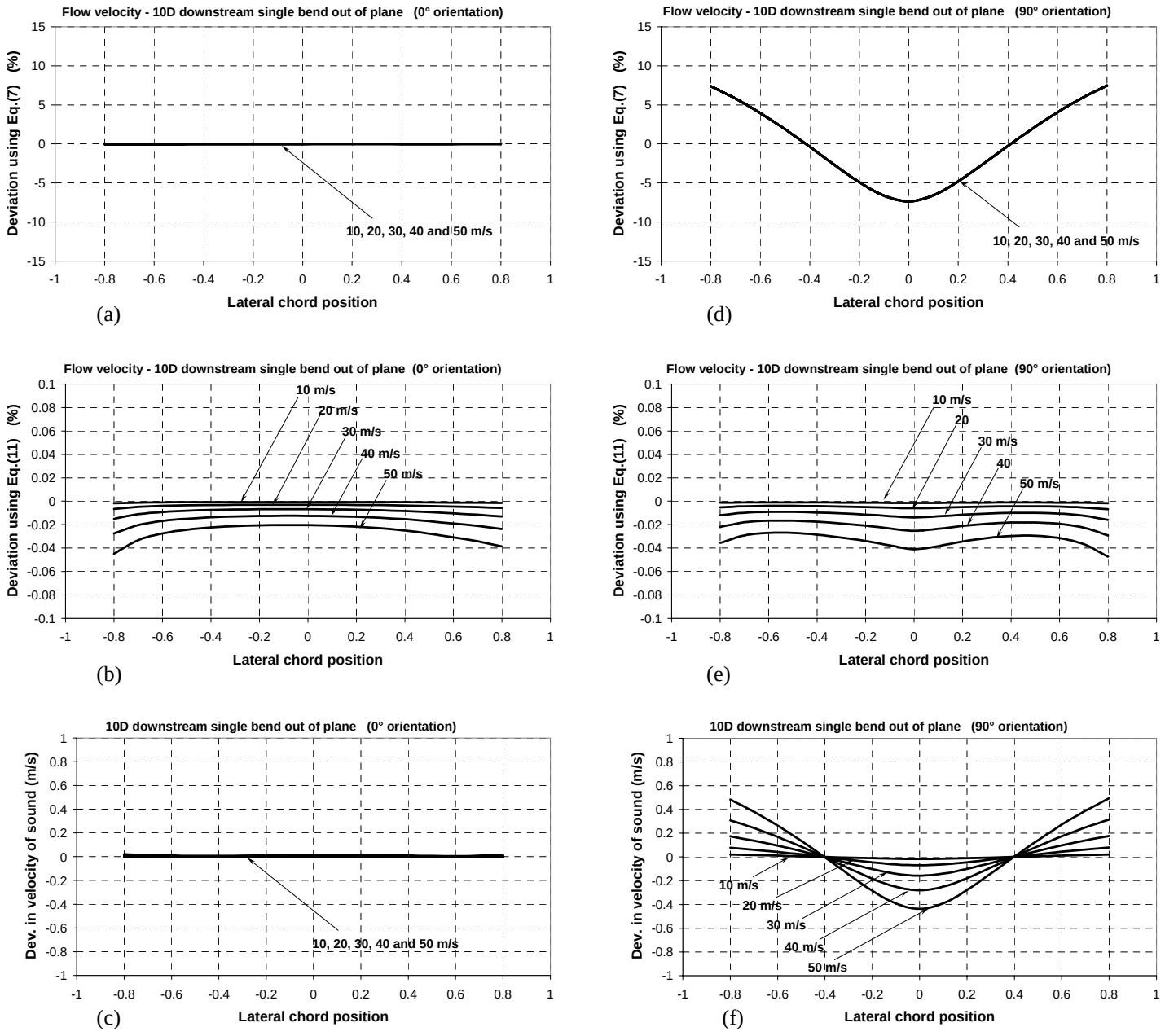

Fig. 9. The effect of asymmetrical axial and transversal flow on the estimate of the average axial flow velocity and VOS, 10D downstream a single 90^o bend, for various lateral chord positions (y/R). Left: 0^o orientation of the USM rel. bend; right: 90^o orientation.

Several observations are made. Firstly, consider the ”measured” average axial flow velocity. A significant effect is found by using Eq. (7), cf. Fig. 9d (90^o orientation of USM rel. to bend). It can be shown that this effect is caused by the transversal flow, and not the asymmetry of the axial flow profile. Fig. 9e shows that by subtracting an assumed uniform-flow transversal flow component (through the geometrical path configuration, or in software, using Eq. (11)), the remaining effect of sound refraction is comparable to the one at straight pipe, for the flow velocities of interest in fiscal metering. For the ”measured” VOS, significant effects are found above 20-30 m/s. These are important both for calculation of density from the measured VOS, and for meter testing by comparison of VOS at different paths.

With respect to meter orientation, the refraction effect due to transversal flow is averaged out over the path at 0^o orientation (Fig.9, left part). However, as illustrated and commented above, this is not the case for 90^o orientation (Fig.9, right part).

5.3 Double 90^o bend out-of-plane - Effects of asymmetrical axial and transversal flow

Fig. 10 shows the deviation from the reference values ($\overline{v}_{i,z}$ and c_i) by using Eqs. (7) and (11) (for flow velocity) and Eq. (9) (for VOS), for various lateral chord positions (*y/R*) and two meter orientations, when the transit times are calculated by ray theory using the CFD calculated profiles shown in Fig. 6b as input to the ray model.

Again, a significant effect is found for the ”measured” average axial flow velocity by using Eq. (7), cf. Figs. 10a and 10d. It can also here be shown that this effect is caused by the transversal flow, and not the asymmetry of the axial flow profile. Figs. 10b and 10e show that by subtracting an assumed uniform-flow transversal flow component (through configuration or in software, using Eq. (11)), the remaining effect of sound refraction is comparable to the one at straight pipe, for the flow velocities of interest in fiscal metering.

For the ”measured” VOS, the effects are even stronger than for the single-bend results shown in Fig. 9, cf. Figs. 10c and 10f. It can be shown that this is caused by the larger transversal flow components, and not the asymmetry of the axial flow profile.

With respect to meter orientation, transversal flow effects are similar for 0^o and 90^o orientation, since the transversal flow is of swirl type.

With respect to inclination angle, other results of the study (not included here) show that the refraction effects of transversal flow on the “measured” *flow velocity* increase significantly with angle, if compensation is not made in the USM (through the geometrical path configuration, or in software, using Eq. (11)). However, if such compensation is made the remaining refraction effects decrease by increasing angle. For the VOS, the error made by using Eq. (9) increases with increasing angle, so that for larger angles than 45^o, these effects become dramatically more significant than in Figs. 9f, 10c and 10f. These results apply both to the single- and double-bend pipe configurations.

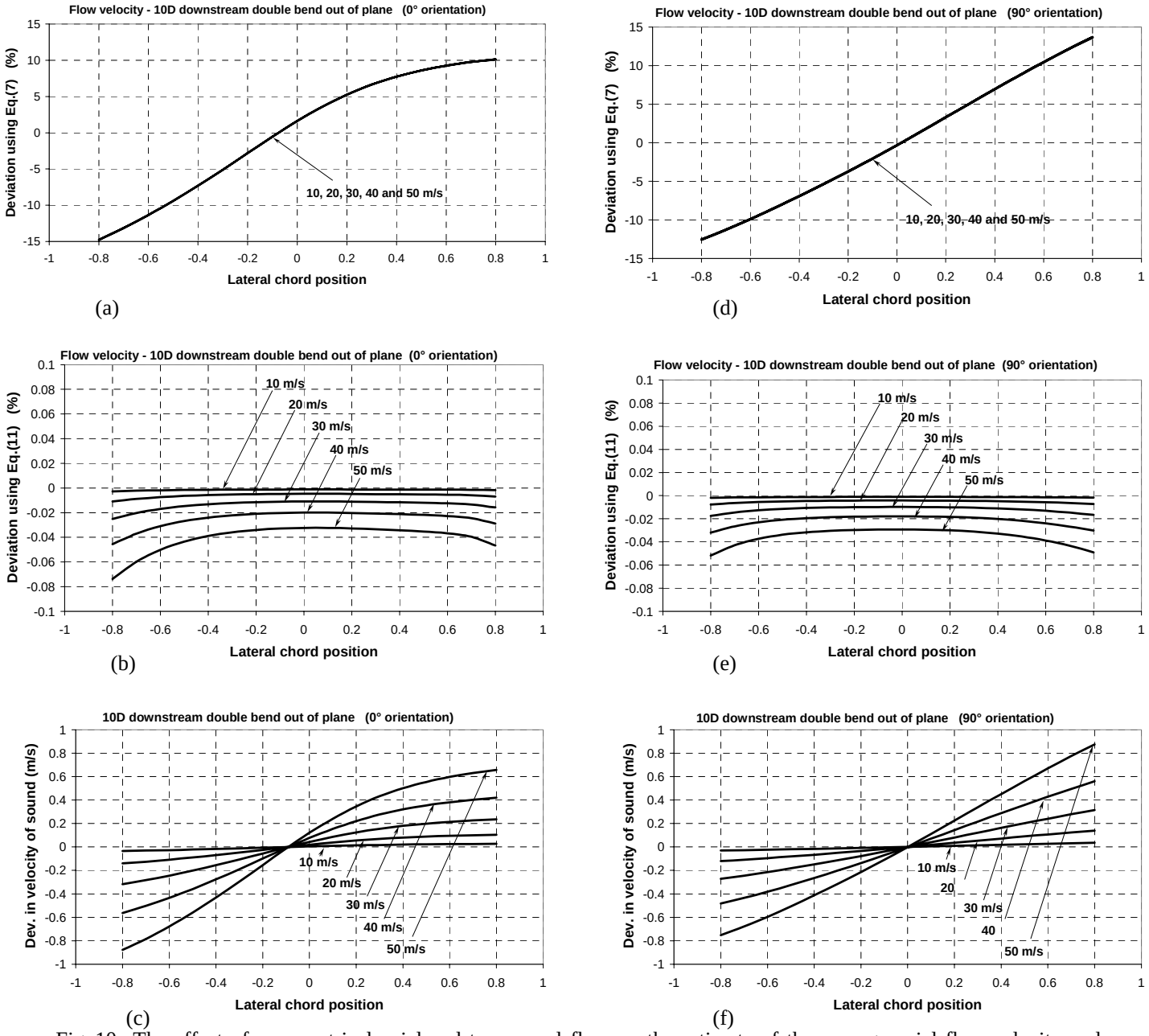

Fig. 10. The effect of asymmetrical axial and transversal flow on the estimate of the average axial flow velocity and VOS, 10D downstream a double 90° bend out-of-plane, for various lateral chord positions (*y/R*). Left: 0° orientation of the USM rel. bend; right: 90° orientation.

6. DISCUSSION AND CONCLUSIONS

An improved theoretical description of sound propagation in moving media may form the basis for further development of USM technology, with reduced systematic errors (not eliminated by flow calibration) and extended application areas (e.g. calculation of gas density and calorific value from the measured sound velocity, VOS).

In the present work a simplified ray theory sound propagation model has been developed and used to address the accuracy of the traditional expressions which are used in present-day USMs for

measurement of the average flow velocity and VOS. The ray tracing method has in addition the potential of improving these methods in current use. Improved expressions are derived which can be employed in the USM methodology (not presented here).

Influences of sound refraction on the axial flow velocity ($\overline{v}_{i,x}$) and VOS have been investigated for flow profiles related to smooth straight pipes (for Reynolds numbers in the range 200-$2.3 \cdot 10^8$) and downstream single and double bends, all calculated using a CFD model.

For the axial flow velocity at a single path ($\overline{v}_{i,x}$), the effects of Reynolds number variation in an ideal straight pipe with symmetrical axial and no transversal flow has been found to be relatively small (e.g. less than 0.1 % for Mach numbers $M_i < 0.1$ and Re > 5000), except for the (relatively rare) combination of very low Reynolds numbers and moderate-to-high Mach numbers. Moreover, for pipes with bends the effects of asymmetrical axial flow are found to be small. Effects of non-uniform transversal flow are small, provided compensation for uniform transversal flow is made in the USM (either by configuration or software).

Consequently, the results of the study indicates that Eq. (11), which has been derived for the simplified case of uniform axial and transversal flow, should be sufficiently accurate for measurement of the axial flow velocity along path no. *i*, for a wide range of symmetrical and asymmetrical axial and transversal flow profiles, at low and moderate flow velocities.

For VOS, the effects of Reynolds number variation in an ideal straight pipe with symmetrical axial and no transversal flow have been found to be relatively small (e.g. less than 0.05 m/s for Mach numbers $M_i < 0.1$ and Re > 5000), except for the (relatively rare) combination of very low Reynolds numbers and high Mach numbers. Moreover, for pipes with bends the effects of asymmetrical axial flow is also found to be small, except for "high" flow velocities. In (hypothetical) applications with no transversal flow, thus, the "traditional approach" for VOS, derived for the simplified case of uniform axial and no transversal flow and given by Eq. (9), appears to be sufficiently accurate, for a wide range of axial flow profiles.

However, refraction effects due to *transversal* flow on VOS are shown to be highly significant also at moderate flow velocities. If the average transversal flow velocity at path no. *i* changes from flow calibration to field operation (which may often be the case), this may be an important effect in applications where VOS measured by the USM is used. Methods to correct for such effects are not available in current USMs. The present work indicates that as no significant effect of non-uniformity of transversal profiles has been found, transversal flow profiles can be treated as being uniform. For this case, an improved VOS expression (relative to Eq. (9)) has been derived (not presented here), enabling correction for transversal-flow effects on VOS provided an estimate of the average transversal flow velocity over the path is available (which is the situation for some USMs [8]).

One common application is the use of VOS for quality control of the USM. If the average transversal flow velocity changes from path to path (which may be the typical situation), the measured VOS will be different from path to path due to measurement error caused by transversal flow, unless the transversal flow effects on the transit times are corrected for. This may cause problems in the quality control of the USM, and may be misinterpreted e.g. to be caused by temperature gradient effects in the gas.

VOS errors at individual paths will propagate into the average VOS calculated for the USM, with consequences for other applications, such as the use of VOS as input to VOS correction of vibrating

element densitometers. In more recent applications where the VOS is used to calculate the gas density and calorific value, a correction of the VOS for sound refraction effects due to transversal flow profile effects may be needed when high accuracy in these quantities is required.

Two parameters (P_v and P_c) have been defined which, - for turbulent flow profiles in straight pipes, may be used to approximately evaluate the importance of the effect of symmetrical axial profiles on the measured flow velocity and VOS, cf. Eq. (18). The above results indicate that these parameters may also be used for asymmetrical axial flow profiles (e.g. for in pipes with bends), - and for the flow velocity also in case of transversal flow.

The flow profile effects on transit times are demonstrated here for USM with non-reflecting paths ($N_{refl,i} = 0$ for all i). For USMs employing reflecting paths ($N_{refl,i} > 0$), it can be shown that the transit time effects will be equal to those in a non-reflecting path USM, provided the axial profile is symmetrical, the transversal flow is a symmetrical swirl, and the flow profiles are constant over the length of the USM. However, such flow profiles are seldom met in practice. Consequently, for reflecting-path USMs, deviations from the above numerical calculations may be expected for realistic flow profiles. Whether these deviations will be higher or lower than in Figs. 8-10 has not been addressed in the investigation reported here. However, evaluation of the detailed influences on USMs with reflecting paths can be made for arbitrary axial and transversal flow profiles (analytical, CFD calculated or experimental) using the ray theory simulation program developed here.

The present results are based on a 2-dimensional ray theory description of sound propagation (cf. Section 3). Preliminary investigations by the authors on extending the ray propagation model to a 3-dimensional description indicate that such an extension may not bring significantly new results into the discussion, so that within the limitations of the ray approach, the above results may be expected to be representative.

More important may be the fact that ray theory description of sound propagation *itself* is restricted, due to the high-frequency approximation inherent in that methodology (cf. Section 3). Since ray propagation models are not able to account for finite-beam and diffraction effects, they represent a simplified treatment of the problem. To fully evaluate the systematic transit time effects discussed here, and other systematic effects (cf. Table 1 and e.g. [12,10]), a more comprehensive analysis based on wave theory will be needed, accounting for acoustic diffraction effects, finite beam interaction with the flow, transducer time delay, pressure and temperature effects on transducers, etc. On the other hand, the relatively simpler approach used here is still considered to represent an improvement relative to current USM methodology, and is motivated by the insight and improved analytical expressions which are obtained using this approach.

ACKNOWLEDGEMENTS

The CFD flow velocity profiles used as one input to the study were calculated using the *MUSIC* code developed by senior scientist Anders Hallanger, CMR. The work has been partially supported by the Research Council of Norway.

REFERENCES

[1] "The Daniel SeniorSonic gas flow meter", Brochure, Daniel Flow Products, USA (2000).

[2] "MPU 1200 ultrasonic gas flow meter", Brochure, Kongsberg Offshore AS, Norway (2000).

[3] "Ultrasonic gas flow meters", Brochure, Instromet International N.V., Belgium (2000).

[4] "Regulations relating to fiscal measurement of oil and gas etc.", Norwegian Petroleum Directorate, Stavanger, Norway (January 20, 1997).

[5] "Measurement of gas by multipath ultrasonic meters". Transmission Measurement Committee, Report no. 9, American Gas Association (A.G.A.) (June 1998).

[6] **Boer, A. H.:** "Testresults Krohne 8" ultrasonic flowmeter", Proc. of the North Sea Flow Measurement Workshop 1997, Kristiansand, Norway, 27-30 October 1997.

[7] **Kinghorn, F.:** "Flow measurement research - Does it have a future?", Opening address, *Proc. of 4th Int. Symposium on Fluid Flow Measurement*, Denver, Colorado, USA, June 27-30, 1999

[8] **Lunde, P., Frøysa, K.-E., Fossdal, J. B. and Heistad, T.:** "Functional enhancements within ultrasonic gas flow measurement", Proc. of the 17th North Sea Flow Measurement Workshop, Oslo, Norway, 25-28 October 1999.

[9] **Zanker, K. and Brown, G.:** "The performance of an ultrasonic meter in wet gas service", Proc. of the 18th North Sea Flow Measurement Workshop, Scotland, 24-27 October 2000.

[10] **Lunde, P., Frøysa, K.-E. and Vestrheim, M.:** "Challenges for improved accuracy and traceability in ultrasonic fiscal flow metering", Proc. of the 18th North Sea Flow Measurement Workshop, Gleneagles, Scotland, 24-27 October 2000.

[11] **Lunde, P. and Frøysa, K.-E.:** "Handbook of uncertainty calculations - Ultrasonic fiscal gas metering stations", Prepared by the Norwegian Society of Oil and Gas Measurement, the Norwegian Petroleum Directorate and Christian Michelsen Research AS, Norway. (In preparation, to be available from the Norwegian Society of Chartered Engineers, Oslo.)

[12] *GERG project on ultrasonic gas flow meters, Phase II*. GERG Technical Monograph TM 11 2000, edited by Lunde, P., Frøysa, K.-E. and Vestrheim, M.. Groupe Européen de Recherches Gazières (VDI Verlag, Düsseldorf, 2000).

[13] **Frøysa, K.-E., Furset, H. and Baker, A.:** "Density and ultrasonic velocity calculations for natural gas", CMR report CMR-98-F1002, Christian Michelsen Research, Bergen (1998) (Confidential).

[14] **Lunde, P., Frøysa, K.-E. and Vestrheim, M.: "***GARUSO* - Version 1.0. Uncertainty model for multipath ultrasonic transit time gas flow meters". CMR Report No. CMR-97-F10014, Christian Michelsen Research AS, Bergen (August 1997).

[15] **McCartney, M. L. Mudd, C. P. and Livengood, R. D.:** "A corrected ray theory for acoustic velocimetry". *J. Acoust. Soc. Am.* **65**, 50-55 (1979).

[16] **Frøysa, K.-E. and Lunde, P.:** "A ray theory approach to investigate the influence of flow velocity profiles on transit times in ultrasonic flow meters for gas and liquid", Proc. of *24th Scandinavian Symposium on Physical Acoustics, Ustaoset, Norway, January 28-31, 2001*.

[17] **Pierce, A.D.:** *Acoustics. An Introduction to Its Physical Principles and Applications* (McGraw-Hill, New York, 1981).

[18] **Lighthill, J.:** *Waves in Fluids* (Cambridge University Press, 1978).

[19] **Hallanger, A., Frøysa, K.-E. and Lunde, P.:** "CFD simulation and installation effects for ultrasonic flow meters in pipes with bends", In: *Proc. of MekIT'01, First National Conference on Computational Mechanics, Trondheim 3-4 May 2001* (Tapir Akademisk Forlag, Trondheim, Norway), pp. 147-167. Extended version accepted for publication in *International Journal of Applied Mechanics and Engineering (IJAME)*, **7**(1), 2002.